The 2009 IEEE/RSJ International Conference on
Intelligent Robots and Systems
October 11-15, 2009 St. Louis, USA

Drive Train Design Enabling Locomotion Transition of a Small Hybrid Air-Land Vehicle

Richard J. Bachmann, *Member, IEEE*, Ravi Vaidyanathan, Roger D. Quinn

***Abstract*—Design modifications have improved the durability and performance of a previously developed hybrid vehicle capable of both aerial and terrestrial locomotion. Whereas the original vehicle could fly, land, and crawl in sequence, it suffered from limited durability, as evidenced by catastrophic failure after a small number of landings – two to four depending on the substrate. The two most common failure modes were breakage of the terrestrial locomotion drive servos and separation of components from the fuselage. Evaluation of the original vehicle also identified the need for an autopilot. This further complicated the durability problem by greatly increasing the vehicle's mass, causing larger impulses in high speed landings. The new fuselage design includes a well-defined nacelle to which the propeller motor is securely mounted. All metal DC motors replace R/C servos in the terrestrial drive system, and a slip clutch limits the torque experienced by the motor during landing. The slip clutch comprises an annulus that drives a concentric shaft through three quad profile o-rings. The new 350 gram vehicle has survived eight landings on different substrates with no sign of damage.**

I. Introduction

Insects and birds demonstrate the ability and the need for mobility both in the air and on the ground. Pure terrestrial locomotion may be impractical for small animals because of the distances that must be traveled to search for food and mates. However, pure aerial locomotion is also undesirable because it is impossible to stay airborne indefinitely, and walking is more energy efficient than flying for traveling short distances. Small robots suffer the same constraints and the ability to both fly and walk would represent a generational leap in their capability [1]. Flight permits a vehicle to travel long distances and approach a target area, while crawling permits movement to a more precise location for tasks such as inspection and surveillance. A detailed analysis of the necessary capabilities of various hybrid mobility vehicles is presented in [2].

There are few published works on small vehicles with the stated goal of both aerial and terrestrial locomotion. The Entomopter [3] uses Reciprocating Chemical Muscle [4] to produce flapping motion of its four wings. We are not aware of data on the vehicle's terrestrial capabilities or performance results for either locomotion mode. The recently developed Microglider [5] also locomotes both on the ground and in the air, and implements a biologically-inspired wing-folding mechanism. However, it hops into the air and glides, and is unable fly for extended periods as is the intended purpose of the vehicle described in this paper.

A hybrid mobility vehicle capable of aerial and terrestrial locomotion (Micro Air-Land Vehicle – MALV) was previously demonstrated by our group [6]-[8]. A thorough trade-off analysis [9] indicated 1) carbon fiber construction for durability, 2) a flexible wing for improved aerial stability and 3) wheel-legs for maximum ground terrain mobility. The 30 centimeter long vehicle implemented a 30 centimeter wingspan by 15 centimeter root chord wing fabricated from polycarbonate coated polyethylene with carbon fiber leading edge and reinforcing spars. The fuselage housed the necessary electronics for tele-operation and the terrestrial drive system, comprising two R/C servos modified for continuous rotation and independently controlled for differential steering.

The 118 gram MALV 1 (Fig. 1) had a cruising airspeed of approximately 11 meters per second and a maximum flight time of about 15 minutes, resulting in a maximum round-trip range of about 5 kilometers. Terrestrially, the vehicle could develop a maximum speed of 0.33 meters per second and could surmount obstacles of height 4.4 centimeters.

Fig. 1. First MALV prototype

An evaluation of the first prototype's performance led to the desire for two critical design improvements: semi-autonomous operation and increased durability. The final application envisioned for this vehicle is as an organic resource for military and first responder personnel in situations that preclude remote piloting of the vehicle by the

Manuscript received March 1, 2009. This work was supported in part by the U.S. Air Force under contract FA8651-05-C-0097 and the by the U.S. Special Operations Command-Naval Postgraduate School (USSOCOM-NPS) Field Experimentation Cooperative Program.

R. J. Bachmann is President of BioRobots, LLC, Cleveland, OH 44127 USA (phone: 216-246-0148; fax: 216-368-3007; e-mail: r.j.bachmann@bio-robots.com).

R. Vaidyanathan is with University of Bristol, Bristol BS8 1TH United Kingdom (e-mail: r.vaidyanathan@bristol.ac.uk).

R.. D. Quinn is Arther P. Armington Professor of Mechanical and Aerospace Engineering at Case Western Reserve University, Cleveland, OH 44106 USA (e-mail: rdq@case.edu).

deploying personnel. A survey of COTS autopilots identified the Procerus Kestrel™ autopilot [10] as the lightest available full-function COTS autopilot. The total mass of the autopilot and associated hardware is 62 grams, significant with respect to the 118 grams of the original MALV. In light of this, the wingspan of the new design was increased to 41 centimeters. The increased mass also resulted in the cruising airspeed increasing to 14 meters per second, and the wing loading increasing from 32 N/m^2 to 64 N/m^2. The increase in wing loading precludes the typical flaring maneuver during landing. The overall result of the increased mass and cruising speed was to increase the impulse load during landing. This is counterproductive to the second critical design improvement – increased durability.

Lack of durability was the most significant shortcoming of the first prototype, primarily because it represented multiple hurdles to the field deployment of MALV. Operationally, low durability would result in short vehicle life-span. Due to the characteristics of the vehicle, even the most controlled landing strongly resembles a crash, from a dynamic loading standpoint. For example, video shows that the vehicle decelerates horizontally from 11 meters per second to zero meters per second in less than 0.25 seconds. This corresponds to an acceleration of ~4.5 times the acceleration of gravity and an average braking force of 5 Newtons. This example is for landing on asphalt only. Landings on gravel and grass resulted in much shorter deceleration times, and therefore higher average decelerations. Furthermore, the vertical deceleration is nearly instantaneous. To make matters worse, the maximum force experienced in an impact is higher than the average impulse load.

This impulse loading is why testing of the first prototype demonstrated that the vehicle could survive only a limited number of deployments. The review panel agreed that, for MALV to gain acceptance among military and emergency personnel, the durability of the vehicle would need to be improved. In addition to adversely affecting the acceptance of MALV, low durability made it difficult to field each vehicle on an individual basis. The "hand-crafted" fabrication and assembly process associated with MMALV requires that each vehicle undergo several trim flights. During this process, controller settings and vehicle control surfaces are adjusted to produce the desired flight characteristics, specifically straight, level flight when the elevator and rudder control inputs are zero. Variations between distinct vehicles caused very different initial flight characteristics between those vehicles, often resulting in crashes on the first trim flight. Due to low durability, these crashes often resulted in damage.

II. Fuselage Design and Fabrication

The MALV 1 fuselage fabrication technique involved hand machining the fuselage mold from a single piece of epoxy modeling board. The shaping process was carried out on a band saw and a belt sander. Whereas this process is quick and results in smooth flowing contours from nose to tail, the process precludes the inclusion of concave surfaces on the fuselage. As a result, the methods by which the propeller motor and control servos were mounted were insufficiently durable to consistently withstand crashes and high impulse landings. A slot of width 0.7 times the motor diameter was hand cut into the top of the fuselage nose. The motor was laid into the slot, and a bead of cyanoacrylate (CA) glue was applied to the resulting line contact on either side of the motor. The control servos were attached to the inside rear of the fuselage with a combination of CA glue and thread. Two holes were drilled in each side of the fuselage. Kevlar thread was woven in one hole, around the servo body, and out the other hole on the same side. This process was repeated several times. Once the servo body was pulled snug against the fuselage wall, a couple drops of CA glue were applied to the contact surface.

The final design includes a conspicuous motor nacelle (Fig. 2). The front face of the fuselage provides a strong, fixed surface on which to mount the propeller motor. This provides significant durability to the mounting system. In fact, a 350 gram prototype of the final design crashed nose first into the ground at full speed, and the motor remained securely attached to the nacelle. A portion of the nacelle is cut away to assist in motor mounting, and to provide cooling airflow over the motor. The speed controller is wired directly to the motor, and resides in the back portion of the motor nacelle. Fig. 3 shows a rendering of the tail boom and control servo mounting bracket that prohibit separation of the control servos during crashes.

Fig. 2. Close-up of the motor nacelle and mounting face

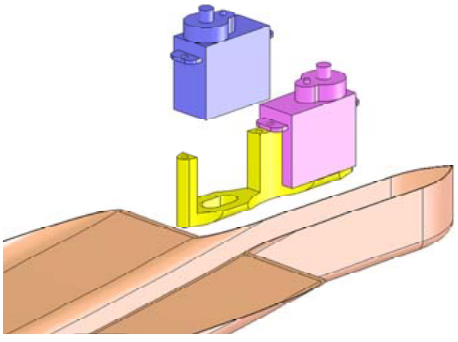

Fig. 3. Close-up of the tail boom, servo mounting bracket, and servos.

III. Terrestrial Drive System Design

Several iterations of wheel-leg drive systems were investigated before a robust combination was identified. Two methods were pursued. First, stronger components were chosen, and second, the biological principle of compliance was implemented. Making components stronger makes them heavier and, in turn, increases impact loads. On the other hand, compliant structures in biological organisms help to reduce damage to mechanical elements during impact, as described by Alexander [11]. Lighter, compliant structures are especially appropriate for aerial vehicles.

The first prototype used an R/C servo, which had been modified to allow for continuous rotation, to drive each wheel-leg. For convenience, this was the first method attempted on MALV 2. The wingspan was increased partly to compensate for the increased mass of the terrestrial drive system. This allowed for the selection of a larger R/C servo. The Blue Bird BMS-380 Max was chosen because it has a metal gear transmission. However, while this did mitigate certain failure modes of the terrestrial running gear, others were found, as shown in Figure 4.

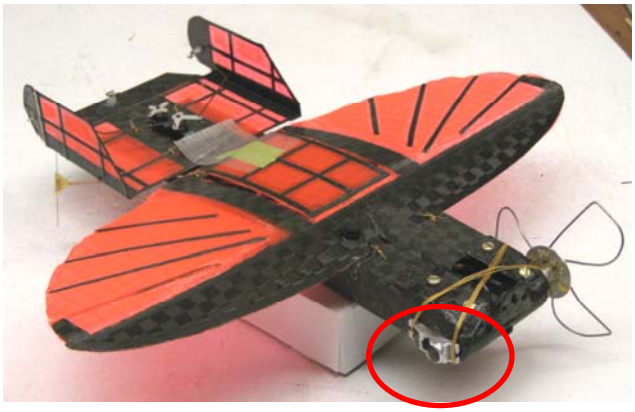

Fig. 4. Even large, metal-geared servos are damaged in landings.

All R/C servo bodies are made of injection molded plastic, which is simply unable to withstand the impulse loads experienced at landing. Therefore, the first step in improving the durability of the system was to replace the R/C servo with a standard DC gearmotor. This requires the addition of a speed controller, and has other drawbacks. Unfortunately, even the best COTS gearmotors are only designed to support a small radial load on the output shaft. For example, on a 10 mm Maxon gearmotor with a 64:1 transmission ratio (a reasonable candidate for the MMALV terrestrial drive system), the recommended maximum radial load on the output shaft is 1531 grams at 5 mm. This corresponds to a 5*g* deceleration for a 300 gram vehicle, which is insufficient to support the impulse load at landing. Furthermore, available gearmotor output shafts tend to be on the order of 1 centimeter long, and there is no way to positively fix an appendage onto the shaft. Considering these characteristics of gearmotors, it was apparent that an indirect drive system would be required.

Figure 5 shows a photo of the initial wheel-leg drive system mounted in a scaled-up version (Model A) of the original fuselage. Early testing confirmed that a timing belt system could successfully transmit motor output torque to the wheel-legs. This system was investigated first for two reasons; it provides high durability, and it offers maximum flexibility on the placement of the gearmotor with respect to the wheel-leg axle. The initial redesigned fuselage, Model A, was insufficiently wide to place the motors end to end, and insufficiently tall to stack the motors. The belt drive system facilitates the nested motor arrangement depicted.

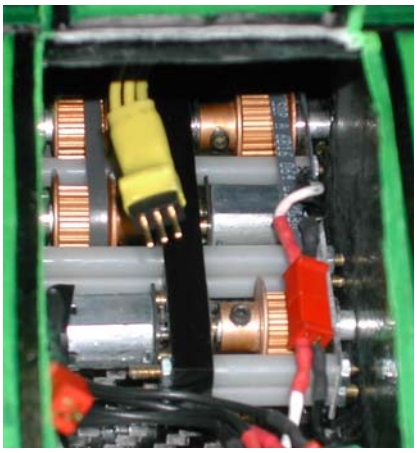

Fig. 5. Initial non-servo terrestrial drive system

While radial loading of the gearmotor output shaft is avoided through this implementation, tangential loading of the wheel-legs is still transmitted to the gearmotor. The candidate motor transmissions have very small gears, which are damaged by large tangential loads experienced during landing. Therefore, the decision was made to implement compliance to limit the torque transmitted from the wheel-legs back to the gearmotor. A preferred torque limit of 120% of the drive gearmotor's stall torque was targeted for a slip-clutch, assuming the transmission has a factor of safety to withstand 20% more than the stall torque.

A. Slip-clutch Hub

Initial implementations of the slip-clutch were carried out at the wheel-leg hubs. In the first design (Figure 6) a soft polymer tube was placed between the wheel-leg axle and the wheel-leg hub. While this arrangement was simple and showed potential during bench tests, it was disqualified by early flight tests. Using the first CNC fuselage (Model B), sequential flight tests were performed. In the initial flight tests, with ballast to simulate the masses of the wheel-leg drive system and the autopilot, the vehicle performed well. However, addition of the wheel-leg drive axles noticeably impaired the vehicle's aerial stability. Furthermore, inclusion of the wheel-leg hubs completely devastated the prototype's controllability. This was likely due to the aerodynamic properties of cylinders. Each 0.5 inch diameter hub produced drag equivalent to a 1 inch thick airfoil 6 inches long, and this drag acted below the CG of the aircraft, making ascent difficult. Also, the shortness of the hub likely

resulted in chaotic vortex shedding, completely disrupting the vehicle's controllability. Furthermore, the target breakaway torque of the system was difficult to obtain because it required unattainable tolerances in the friction material.

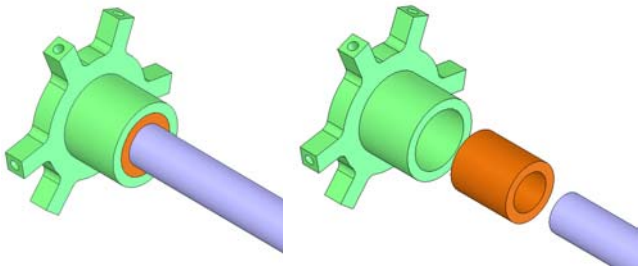

Fig. 6. Slip-clutch hub design assembled (left) and exploded (right)

B. Angled Slip-clutch Hub

A second hub-clutch design (Figure 7) produced a more disk-like hub, rather than the cylindrical hub depicted above. The compressed spring creates a normal contact force between the outer stator (A) and the wheel-leg hub (B), and between the hub and the inner stator (C). The outer pin (D) transmits torque to the outer stator, and holds it onto the end of the shaft, while the inner pin (E) transmits torque to the inner stator. By varying the spring properties and the contact angle between the rotor and the inner stator, the normal force, and the resulting frictional force and breakaway torque of the clutch, could be tuned. However, this design suffered from low durability in subsequent flight tests. Increasing the size of the components to impart the necessary strength would likely have resulted in poor flight characteristics as in the previous method. The decision was made to move the clutch assembly internal to the fuselage.

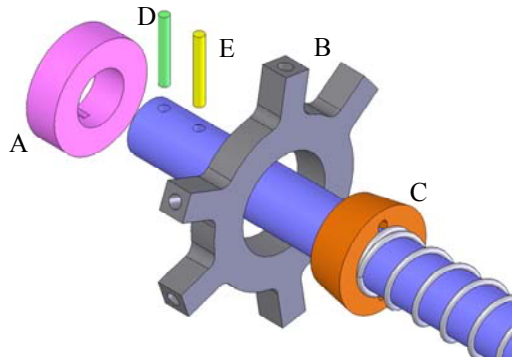

Fig. 7. Exploded view of angled slip-clutch hub design

C. Parallel Shaft O-ring Slip-clutch

1) Test Apparatus

Figure 8 shows a rendering of a test rig for determining the torque transmission capacity of the various torque limiter arrangements. The torque limiter design being tested comprises two parallel, non-concentric spools that contact through a soft polymer material. The first (or drive) spool (shown in red) is connected to the motor output shaft (blue), and the second (or driven) spool (salmon) is connected to the wheel-leg axle (yellow). Decreasing the gap between the drive and driven spools increases the compression of the polymer material (dark gray), resulting in an increase in the contact force, and subsequent increases in the maximum frictional force and torque transmitted between the two spools.

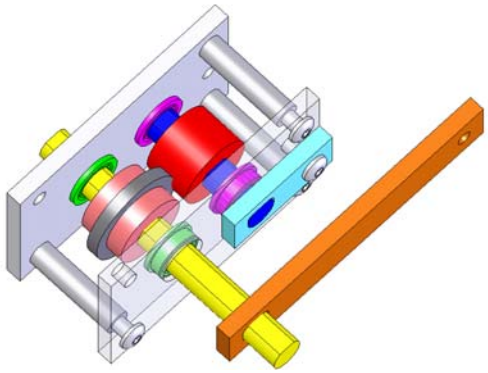

Fig. 8. Test rig for measuring torque limiter transmission capacity

2) Test Procedure for Torque Limiter Evaluation

The design of the test rig was intended to facilitate mimicry of the MALV deployment process. To maximize portability, the wheel-legs should not be attached to the vehicle during storage and transport. However, any assembly required prior to deployment must be convenient and straightforward. One option would be to remove only the wheel-leg. However, this would require a quick-release mechanism, which tends to be bulky, and the resulting hub size would adversely affect the aerial performance of the vehicle. The other option is for the axles to disengage from the drive mechanism during storage and transportation. Once the wheel-leg axle is removed from the driven spool, the polymer material (A) will push the two spools apart, as depicted in Figure 9-1. During pre-deployment assembly, the polymer material must be recompressed using the following steps. The wheel-leg axle (B) is inserted through the outer bearing (C) and into the driven spool (D) (Figure 9-2). A force (F) applied to the outer end of the wheel-leg axle compresses the polymer such that the wheel-leg axle aligns with the inner bearing (E) (Figure 9-3). The axle is then inserted through the inner bearing (Figure 9-4).

The test procedure was as follows (Fig. 9). The motor shaft bearings (G) were inserted into their respective pockets, and the two plates were assembled. The motor shaft (H) was inserted through the bearings and the drive spool (J). The shaft clamp (K) was attached to prevent the motor shaft from rotating. A driven spool (L) was selected, and the diameter of the driven spool recorded. The polymer material was placed on the driven spool. The driven spool was held between the plates while the pre-deployment assembly process, as enumerated above, was performed. Once the test rig was fully assembled, A lever arm was attached to the wheel-leg axle, and progressively heavier weights were

hung from the lever arm until the wheel-leg axle began to rotate, denoting slippage between the polymer and the drive spool. The torque at slippage was recorded.

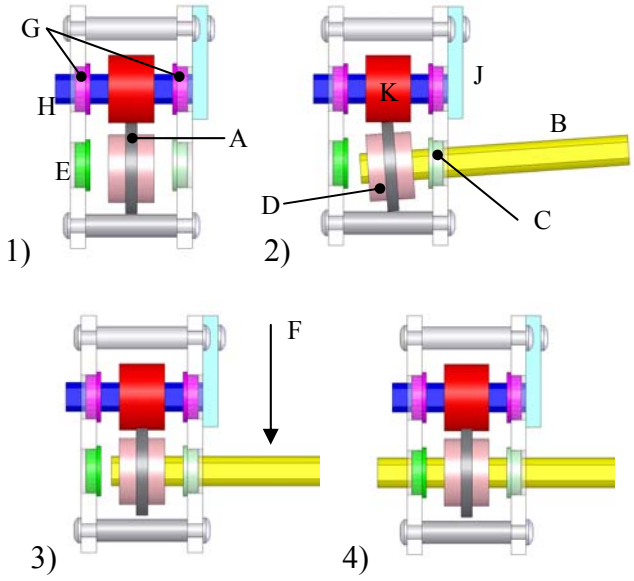

Fig. 9. Schematic representation of pre-deployment assembly process of the wheel-leg axles into the drive system.

Testing revealed the impracticality of this design. The first tests used an o-ring that produced very little interference with the two hubs. The torque delivered by this arrangement was well below the desired torque. As the thickness of the o-ring increased, the torque transmitted by the assembly increased. However, while the transmitted torque was still well below the desired value, the force required to assemble the unit (F in Figure 9-3) became unacceptably high. A slight alteration to this slip-clutch resulted in the final design.

D. Concentric Shaft O-ring Slip-Clutch

Figure 10 shows an assembled view and Figure 11 shows an exploded view of the final design of the terrestrial drive system. Each wheel-leg is powered by a Solarbotics™ GM13a gearmotor (A), which produces 14.9 in-oz of torque at start-up, and 113 rpm under no load. A 26 tooth 48 diametral pitch gear (B) mounted to the motor output shaft adaptor (C) impels a 36 tooth gear (D) that is press fit onto the outer cylinder (E) of the friction clutch mechanism. The clamshell design of the friction clutch outer cylinder eases assembly of the unit. Three 5/16" I.D. x 1/2" O.D. quad-profile o-rings (F) transmit power from the outer cylinder to the inner cylinder (light blue). The normal pressure between the o-rings and the outer cylinder produces a break-away torque of approximately 166% of the motor stall torque (120% magnified by the 36:26 gear ratio). The O.D. of the inner cylinder is sized to produce optimal compression of the three o-rings. The two-piece inner cylinder has internal flats that positively engage the wheel-leg axle (H). The snap ring (J) at the end of the inner cylinder fits into the groove on the wheel-leg axle, allowing for quick attachment and removal of the wheel-leg.

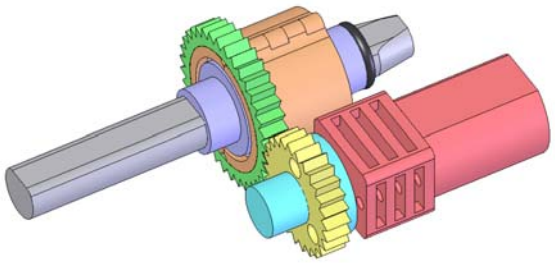

Fig. 10. Assembled view of the terrestrial drive system power train

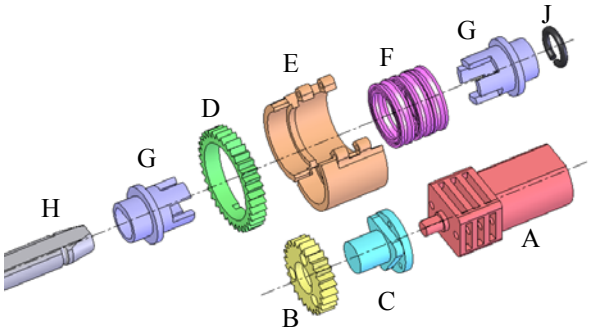

Fig. 11. Exploded view of the terrestrial drive system power train

Figure 12 shows the three piece housing for the final terrestrial drive system. The outer layer (salmon) houses two bearing, one for the output shaft of the motor output shaft adapter and one for the inner cylinder of the slip-clutch mechanism. The large hole in the middle section (blue) encloses the slip-clutch mechanism, and the small hole is a pass-through for the motor output shaft. Not visible from this side is a rectangular pocket behind the motor axle pass-through hole. This pocket fits snugly around the outer end of the transmission on the drive motor, and mates to the rectangular pocket on the inner layer (green). Together, these two pockets secure the motor placement without requiring screws. The inner layer also holds the inner bearing for the inner cylinder of the clutch mechanism. Not shown in the figure is the snap ring housing, which mounts to the in-board side of the inner layer to hold the snap ring in place as the wheel-leg axle is inserted into the mechanism.

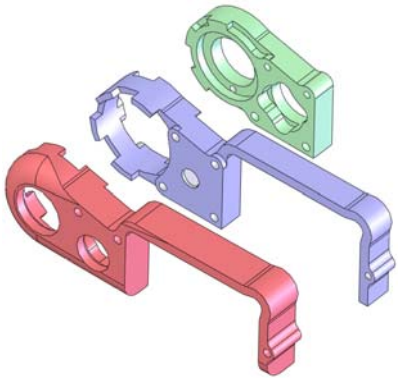

Fig. 12. Exploded view of terrestrial drive system housing

IV. Results and Discussion

A new vehicle (MALV 2 – Fig. 13) was constructed and equipped with the terrestrial drive system depicted in Figures 10 through 12. This vehicle has performed well in eight trials. The first two flights resulted in crash landings in a field of grass approximately 30 centimeters tall. Two subsequent flights on the same day resulted in landings on matted grass approximately 3 centimeters thick. Two flights at a later time resulted in landings on a field with a thin covering of grass. The last two flights resulted in landings that began on asphalt and ended on gravel. The vehicle successfully crawled after the each of the last six flights. No repairs were performed on the vehicle, and the terrestrial drive system was inspected and no damage was found. The combination of strengthened components and judicious use of compliance in the drive train solves the problem of durability and results in a viable small vehicle that can fly long distances, land, and crawl on the ground.

Fig. 13. Robust MALV

Figure 14 shows a sequence of frames captured from a video of MALV 2 flying, landing, and crawling.

Fig. 14. Upper-left: MALV 2 climbs to cruising altitude after hand launch. Upper-right: MALV 2 approaches for a landing. Lower left: MALV 2 at the landing point. Lower-right: MALV 2 crawling away from the landing point. The dot 'A' is stationary with respect to ground.

Take-off from the ground has not been attempted with MMALV 2, but prior experience [6] strongly suggests that the vehicle will be able to gain flight by walking off the top of a building. A similar vehicle has also been able to take-off from the ground on concrete, using the wheel-legs as skids. While wheels may decrease the "runway" required for this type of take-off, experiments demonstrate that neither wheels nor wheel-legs allow the vehicle to take-off on grass.

MALV 2's performance characteristics are summarized in Table 1.

Parameter	Value
Total mass	365 g
Cruising air speed	14 m/s
Maximum flight time	12 min
Maximum terrestrial speed	0.33 m/s
Maximum obstacle height	3 cm

Table 1. Performance characteristics of MALV II.

References

[1] http://www.acq.osd.mil/sadbu/sbir/solicitations/sbir041/af041.htm AF04-177.

[2] Bachmann, R.J., F.J. Boria, P.G. Ifju, R.D. Quinn, J.E. Kline, R. Vaidyanathan, "Utility of a Sensor Platform Capable of Aerial and Terrestrial Locomotion," Proceedings of the IEEE/ASME International Conference on Advanced Intelligent Mechatronics (AIM2005), Monterey California, July, 2005.

[3] Ayers, J., J.L. Davis, A. Rudolph (eds.), Neurotechnology for Biomimetic Robots, The MIT Press, pp 481-509.

[4] Michelson, R., D. Helmick, S. Reece, C. Amareno, "A Reciprocating Chemical Muscle (RCM) for Micro Air Vehicle "Entomopter" Flight," AUVSI'97, Proceedings of the Association for Unmanned Vehicle Systems International, July 1997.

[5] Zufferey, J.-C., A. Klaptocz, A. Beyeler, J.-D. Nicoud, D. Floreano, "A 10-gram Vision-based Flying Robot," *Advanced Robotics*, 21(14):1671-1684, 2007.

[6] Boria, F.J., R.J. Bachmann, P.G. Ifju, R.D. Quinn, R. Vaidyanathan, C. Perry, J. Wagener, "A Sensor Platform Capable of Aerial and Terrestrial Locomotion," Proceedings of IEEE/RSJ 2005 International Conference on Intelligent Robots and Systems (IROS2005), Edmonton, Alberta, Canada, 2-6 August 2005.

[7] Bachmann, R.J., R. Vaidyanathan, F.J. Boria, J. Pluta, J. Kiihne, B.K. Taylor, R.H. Bledsoe, P.G. Ifju, R.D. Quinn, "A Miniature Vehicle with Extended Aerial and Terrestrial Mobility," in Flying Insects and Robots, D. Floreano, J.-C. Zufferey, M. Srinivasan, C. Ellington, eds. 2008.

[8] Bachmann, R.J., F.J. Boria, R. Vaidyanathan, P.G. Ifju, R.D. Quinn, "A biologically inspired micro-vehicle capable of aerial and terrestrial locomotion," *Mechanism and Machine Theory*, Vol. 44, No. 3, pp. 513-526.

[9] Bachmann, R.J., A Hybrid Vehicle for Aerial and Terrestrial Locomotion, Ph.D. Dissertation, Case Western Reserve University, Cleveland, OH, 2009.

[10] Procerus Technologies (http://www.procerusuav.com/), "Kestrel Installation and Configuration Guide," May 2006.

[11] Alexander, R.McN. "Three Uses for Springs in Legged Locomotion," *International Journal of Robotics Research* 9:2, 1990.